

1 **Charging Effect on the 80-200 nm Size Atmospheric Aerosols during**
2 **a Lightning Event**

3
4 **Hong-Ku Lee¹ and Kang- Ho Ahn***

5
6 ¹*Department of Mechanical Engineering, Hanyang University, Seoul, 04763, R. of Korea.*

7 ^{*}*Department of Mechanical Engineering, Hanyang University, Ansan, 15588, R. of Korea.*

8
9 **Abstract**

10
11 Atmospheric aerosol charging is caused mainly by cosmic rays and/or natural radioactive
12 material decay. Because the ionization process generates well-balanced ion pairs, positive and
13 negative ions in the air are at almost the same concentrations. The atmospheric aerosol electrical
14 charge is therefore usually neutral. We measured the particle charge polarity distribution in the
15 atmosphere during a lightning event at ground level. We found that the 80 – 200 nm particle
16 charge balance during a lightning event was skewed either to the positive or the negative.
17 Furthermore, the particle charge polarity changed very rapidly (within a few minutes) from
18 negative to positive or vice versa. There was also a two-fold higher charged particle fraction
19 during a lightning period than a normal day. This increased charged particle fraction may
20 decrease the total particle concentration in the atmosphere by deposition on raindrop surfaces.

21
22 **Keywords:** Atmospheric particle charging, Charging polarity reversal, Lightning effect, Charged
23 cloud

24

^{*} Corresponding author. Tel: +82-31-417-0601; Fax: +82-31-436-8184

E-mail address: khahn@hanyang.ac.kr

25 INTRODUCTION

26

27 There have been numerous research reports on atmospheric aerosol effect on climate, visibility,
28 human health and so on (Ulrich Pöschl, 2005). The atmospheric aerosol plays a very important
29 role in cloud formation and the radiative energy budget of the Earth (Andreae and Rosenfeld,
30 2008; IPCC, 2007). Usually, particles in the air are in an electrically neutral state. If particles are
31 charged, the charged particles can scavenge aerosols by coagulation and their rate of deposition
32 on surfaces may be increased and also enhance ice particle formation in a cloud (Tinsley et al.,
33 2000). Atmospheric particles are usually charged by galactic cosmic rays (GCRs) and/or
34 radioactive material decay from soil (Reist, 1993). Because GCRs and/or radiation generate an
35 almost equal number of positive and negative ions in the air, atmospheric particles are usually in
36 a neutrally charged state. Charged atmospheric particles may also affect human health because
37 the deposition of charged particles in human lungs is enhanced compared to that of uncharged
38 particles (Fews, et al., 1999). Some researchers have reported that the atmospheric aerosol can
39 enhance lightning activity (Yuan et al., 2001; Naccarato et al., 2003; Kar et al., 2009). However,
40 no report on atmospheric aerosol charge phenomena related with a lightning has been published.

41 Laakso et al. (2007) developed an instrument incorporating a differential mobility analyzer
42 (DMA) (Winklmayr et al., 1991) to classify the charged ultra-fine particles and a condensation
43 particle counter (CPC) (Stolzenburg and McMurry, 1991) to measure new particles formed by

44 ion-induced nucleation. However, this instrument is not suitable for measuring rapidly changing
45 aerosol charging states because of the electrical scanning time of the DMA.

46 In this research, we monitored the charging state of the atmospheric aerosol and its particle
47 charging characteristic during a lightning event on the ground. To monitor the charging
48 characteristics of the atmospheric aerosol, we used the aerosol electrical mobility spectrum
49 analyzer (AEMSA) devised by Ahn and Chung (2010). The AEMSA can detect the electrical
50 mobility spectrum of charged single particles in the nano-meter size range, regardless of their
51 polarity, without electrical scanning.

52 53 **METHODS**

54
55 Measurements were performed at Hanyang University, Ansan, R. of Korea and the aerosol
56 sampling system was housed in the 4th floor laboratory of the 5th Engineering Building. The
57 sampling site, marked as the concentric circle in Fig. 1 is located near the west coast of the
58 Korean Peninsula. Precipitation was measured every 30 minutes using AWS (Davis Instruments,
59 Vantage pro2) at the sampling site. The lightning event was measured with polarity, magnitude,
60 type (cloud-to-ground : CG, cloud-to-cloud : CC) and location (Krider et al., 1980). The lightning
61 event and cloud coverage data were provided by the Korea Meteorological Administration
62 (KMA). The lightning events recorded only within the broken line circle with a radius of 10 km
63 shown in Fig. 1 were used in this study.

64 We built the sampling system shown in Fig. 2 to measure the charging state of atmospheric
65 particles. Atmospheric particles are sampled through an OD 12.5 mm and a 1.5 m long copper
66 tube. To minimize particle loss in the sampling tube, the sampling air is pumped at a flow rate of
67 20 lpm with a vacuum pump and a small portion of sampling air (0.4 lpm) is extracted and
68 introduced into the AEMSA for particle charge analysis. To prevent the charged particle loss
69 inside the sampling tube, an electrically conductive copper tube is used. The main sampling flow
70 (20 lpm) is monitored with a rotameter, and the AEMSA flow (0.4 lpm) is controlled with a mass
71 flow controller (MFC). We applied an analyzing voltage of 1,500 V to the AEMSA. This
72 electrical potential allows the detection of particles with an electrical mobility ranging from 3.945
73 $\times 10^{-8} \text{ cm}^2 \text{ V}^{-1} \text{ s}^{-1}$ to $1.027 \times 10^{-8} \text{ cm}^2 \text{ V}^{-1} \text{ s}^{-1}$. Assuming that a particle is singly charged, this
74 corresponds to particles with a diameter of from 80 nm to 200 nm. The AEMSA was installed
75 inside the laboratory window and the sampling probe was projected outside of the window. The
76 total length of the sampling probe was 1.5 m and the end of probe was 1 m away from the window.
77 AEMSA measures particle charge and size distribution every second. However, when the particle
78 concentration is not high enough like a clean day, 1 second data does not give statistically
79 meaningful results. To overcome this problem we accumulated the data for 5 minutes to reduce
80 statistical error. The raw AMESA data are shown in Fig. 3. A positively charged particle in the
81 AEMSA yields a corresponding count on the left side of the graph. Smaller charged particles are

82 detected further away from the center pixel. Non-charged particles are detected at the center pixel.
83 However, the finite dimensions of a particle-introducing nozzle, the spread of signals in the
84 AEMSA for the same electrical mobility particle is inevitable. To find a relationship between the
85 particle electrical mobility and the AEMSA detection pixel position a calibration process is
86 needed. The AEMSA system was calibrated with known size particles generated by the DMA.
87 The detected position of particles with a single charge is labeled on the upper x-axis in Fig. 3
88 (Ahn and Chung, 2010).

89

90 **RESULTS AND DISCUSSION**

91

92 Some of the measurement results obtained on October 15th, 2011 are shown in Fig. 3 and there
93 was a very severe thunder storm as shown in Fig. 4(a). A typical atmospheric aerosol charge
94 distribution is shown in Fig. 3(a) and it shows that the number of positively and negatively
95 charged atmospheric particles are fairly well balanced. However, when the thunderstorm passes
96 over the sampling site, the atmospheric aerosol charge balance shifted and the populations of
97 negatively charged particles increased, as shown in Fig. 3(b). About four minutes later, the
98 positively charged particle count increased dramatically (Fig. 3(c)). This polarity reversal
99 phenomenon continued until the thunderstorm had moved away from the sampling site. This may

100 imply that a strong electric field was formed between the cloud and ground to break the particle
101 charge balance and the particle charge reversal phenomena may cause by the electrical field
102 formation between the cloud and the ground. This atmospheric aerosol charge polarity reversal
103 phenomena is very similar to the observation of atmospheric electric field change reported by
104 Moore and Vonnegut in 1977. They took measurements on the ground beneath a thunderstorm.
105 Based on their report and our measurement, it is believed that the atmospheric aerosol charging
106 during lightning is strongly related with the electric field between the thunder cloud and the
107 ground. The charged particle polarity ratio (N_+ / N_-), precipitation, and two types of lightning
108 events from October 15th to 16th, 2011 are shown in Fig. 4(a). Precipitation was plotted by simple
109 bar graph along with right y-axis. The types of lightning were distinguished by cross (CC : cloud
110 to cloud) and star (CG : cloud to ground) symbols. Polarity and magnitude of lightning were
111 plotted along with offset y-axis on the right side of the graph.

112 On the stormy days of Fig. 4(a) and Fig. 5 (a), (b), a strong charged particle polarity ratio
113 fluctuation was observed. The fluctuation was almost coincident with the lightning event.
114 However, on clear days, the atmospheric particle charge balance is close to 1, as shown in Fig.
115 4(b). This phenomenon also has been observed from 2011 to 2016 on clear days. Fig. 5(a) and (b)
116 are one of the representative measurements in summer and winter season. From these

117 measurements, we can deduce that the thunderstorm has a strong effect on atmospheric particle
118 charge balance regardless of seasonal variation.

119 Lightning generates vast numbers of ion pairs, some of which will be separated in the strong
120 electric field and increases the electrical conductivity of cloud temporarily. Then, on a stormy day,
121 the charge distribution of thunder cloud can be changed easily. The ratio of charged particles, N_+
122 $+ N_-$, to total detected particles, $N_t = N_0 + N_+ + N_-$, was calculated and the curve that was plotted
123 is shown in Fig. 6. The charged particle ratio ranged from 13.7 % to about 66.9 % on the stormy
124 days, such as Oct. 15 – 16th, 2011 (Fig. 6(a)). However, on the clear days of Oct. 18 – 19th, 2011,
125 the charged particle population was very stable and ranged from 19.3 % to 36 %, as shown in Fig.
126 6(b). The mean value and standard deviation of charged particle ratio in Fig. 6(a) were 39.42 %
127 and 9.3 %. In Fig. 6(b), they were 27.36 % and 4.2 %. These two graphs clearly show that
128 thunderstorms can enhance the charged particle population in the atmosphere near the ground.

129 The interior of thunder cloud contains a bipolar charge distribution consisting of positive
130 charge in the upper part of the cloud and negative charge below the positive (Geophysics Study
131 Committee et al., 1986). Usually, lower negative charge causes CG lightning with negative
132 polarity (-CG) and upper positive charge cloud causes CG lightning with positive polarity (+CG).
133 Generally, when the thunder cloud causes +CG lightning comes near, the ground is polarized as
134 negative and positively charged particles are concentrated near the ground. Then, the charged

135 particle polarity ratio (N_+ / N_-) increases larger than 1 and vice versa. Fig. 7 shows correlation
136 with CG lightning events polarized by same polarity for more than 5 minutes and its charged
137 particle polarity ratio from 2011 to 2016. In Fig. 7, most of the charged particle polarity ratio
138 corresponding to positive lightning shows the charged particle polarity ratio value greater than 1
139 and vice versa except a few cases. From this plot, we may deduce that when the ground is
140 polarized by thunder cloud, the number of particle charged by opposite polarity increases near the
141 ground.

142 Fig. 8 illustrates the mechanism of charged particle imbalance phenomenon near the ground.
143 Charged particle imbalance is mainly caused by the electrical field induced by the thunder cloud
144 and the cloud nearby that may carry induced charges too. As a result, the charged particle polarity
145 ratio is changing by the polarity of thunder clouds and by the following clouds passing over the
146 test site. These moving clouds by the wind will give the charged particle polarity oscillation
147 phenomena for the fixed ground monitoring station. Therefore, on a stormy day, a substantial
148 charge imbalance may often be observed without a lightning, as shown in Fig. 4(a).

150 **CONCLUSIONS**

151

152 For the first time, we successfully monitored the charge of atmospheric particles during the
153 thunderstorm events. We found that the atmospheric particles were usually in the neutral state on
154 clear days. However, when a thunderstorm passed, the aerosol charge balance was strongly

155 disturbed and as a result a rapid particle charge polarity fluctuation was observed. Under
156 thunderstorm conditions, the charged particle population in the air was two-to three-fold higher
157 than that observed on clear days. We also found that the thunderstorm clouds could strongly
158 influence on the atmospheric aerosol charging and the particle charge polarity near the ground.

159

160 **ACKNOWLEDGMENTS**

161

162 This work was supported by the Korean Ministry of Environment as an "Eco-innovation
163 project". The authors are greatly acknowledged KMA providing the lightning data.

164

ACCEPTED MANUSCRIPT

165 **REFERENCES**

166

167 Ahn, K.H.; Chung H. Aerosol Electrical Mobility Spectrum Analyzer. *J. Aerosol Sci.* **2010**, *41*
168 (4), 344–351, DOI: 10.1016/j.jaerosci.2010.01.005.

169 Andreae, M. O.; Rosenfeld, D. Aerosol-cloud-precipitation interactions, Part 1. The nature and
170 sources of cloud-active aerosols, *Earth-Science Reviews*, **2008**, *89* (1), 13-41, DOI:
171 10.1016/j.earscirev.2008.03.001.

172 Fewes, A. P.; Henshaw, D. L.; Wilding , R. J.; Keitch, P. A. Corona ions from power lines and
173 increased exposure to pollutant aerosols, *Int. J. Radiat. Biol.*, **1999**, *75* (12), 1523-1531, DOI:
174 10.1080/095530099139124.

175 Summary for Policy makers. *In: Climate Change 2007: The Physical Science Basis. Contribution*
176 *of Working Group I to the Fourth Assessment Report of the Intergovernmental Panel on Climate*
177 *Change; IPCC : Cambridge University Press, Cambridge, United Kingdom and New York, NY,*
178 *USA.; 2007; <http://www.ipcc.ch/pdf/assessment-report/ar4/wg1/ar4-wg1-spm.pdf>*

179 Kar, S. K.; Liou, Y. -A.; Ha, K. -J. Aerosol effects on the enhancement of cloud-to-ground
180 lightning over major urban areas of South Korea, *Atmospheric Research*, **2009**, *92*, 80-87, DOI:
181 10.1016/j.atmosres.2008.09.004.

182 Laakso, L.; Gagne, S.; Petaja, T.; Hirsikko, A.; Aalto, P.P.; Kulmala, M.; Kerminen, V.-M.
183 Detecting charging state of ultra-fine particles: instrumental development and ambient
184 measurements, *Atmos. Chem. Phys.*, **2007**, 7 (5), 1333-1345, DOI: 10.5194/acp-7-1333-2007.

185 Moore, C. B.; Vonnegut, B. *The Thundercloud, in Lightning*, Vol. 1, R. H. Gold, ed.; Academic
186 Press: New York, 1977.

187 Naccarate, K. P.; Pinto Jr., O.; and Pinto, I.R.C.A. Evidence of thermal and aerosol effects on the
188 cloud-to ground lightning density and polarity over large urban areas of Southeastern Brazil,
189 *Geophys. Res. Lett.*, **2003**, 30 (13), 1674, DOI: 10.1029/2003GL017496.

190 Reist, P. C. *Aerosol Science and Technology*, 2nd, ed.; McGraw-Hill Inc., 1992.

191 Stolzenburg, M. R.; McMurry, P. H. An ultrafine aerosol condensation nucleus counter, *Aerosol*
192 *Sci. Technol.*, **1991**, 14 (1), 48-65, DOI: 10.1080/02786829108959470.

193 Tinsley, B. A.; Rohrbaugh, R. P.; Hei, M.; Beard, K. V. Effects of Image Charges on the
194 Scavenging of Aerosol Particles by Cloud Droplets and on Droplet Charging and Possible Ice
195 Nucleation Processes, *J. Atmos. Sci.*, **2000**, 57, 2118 – 2133, DOI: 10.1175/1520-
196 0469(2000)057<2118:EOICOT>2.0.CO;2.

197 Winklmayr, W.; Reischl, G.P.; Linder, A.; Berner, A. A new electromobility spectrometer for the
198 measurement of aerosol size distributions in the size range from 1 to 1000 nm, *J. Aerosol Sci.*,
199 **1991**, 22 (2), 289-296, DOI: 10.1016/S0021-8502(05)80007-2.

200 Yuan, T.; Remer, L. A.; Pickering, K. E.; Yu, H. Observational evidence of aerosol enhancement
201 of lightning activity and convective invigoration, *Geophys. Res. Lett.*, **2011**, 38, L04701, DOI:
202 10.1029/2010GL046052.

203 Griffiths, R. F. Corona Charging of Frozen Precipitation, *J. Atmos. Sci.*, **1976**, 33, 1602 – 1606,
204 DOI: 10.1175/1520-0469(1976)033<1602:CCOFP>2.0.CO;2.

205 Qie, X. S.; Zhang, Y.; Yuan, T.; Zhang, Q.; Zhang, T.; Zhu, B.; Lu, W.; Ma, M; Yang, J.; Zhou,
206 Y.; Feng, G. A review of atmospheric electricity research in China. *Adv. Atmos. Sci.*, **2015**, 32 (2),
207 169–191, DOI: 10.1007/s00376-014-0003-z.

208 Geophysics Study Committee, Geophysics Research Forum, Commission on Physical Sciences,
209 Mathematics and Resources, Commission on Physical Sciences, Mathematics, and Applications,
210 Division on Engineering and Physical Sciences, National Research Council; *The Earth's*
211 *Electrical Environment*; The National Academies Press: Washington, D.C., 1986.

212 Ulrich Pöschl. Atmospheric Aerosols: Composition, Transformation, Climate and Health Effects,
213 *Angewandte Chemie International Edition*, **2005**, 44 (46), 7520-7540, DOI:
214 10.1002/anie.200501122.

215 Krider, E. P.; Noggle, R. C.; Pifer, A. E.; Vance, D. L. Lightning direction finding systems for
216 forest fire detection, *Bull. Amer. Meteor. Soc.*, **1980**, 9 (61), 980-986, DOI: 10.1175/1520-
217 0477(1980)061<0980:LDFSFF>2.0.CO;2.

218

ACCEPTED MANUSCRIPT

Figure Captions

219

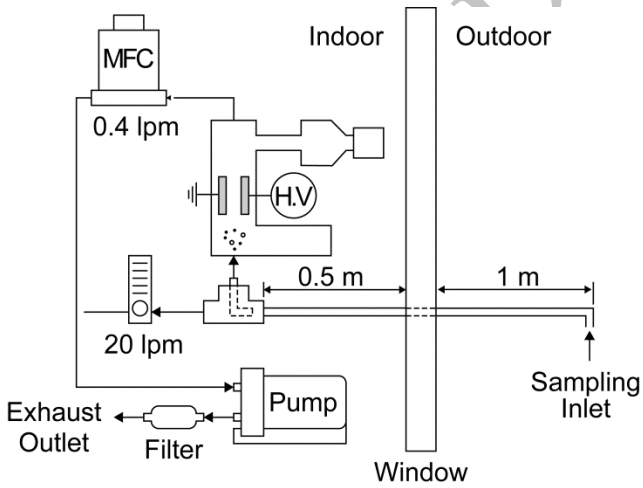
220



221

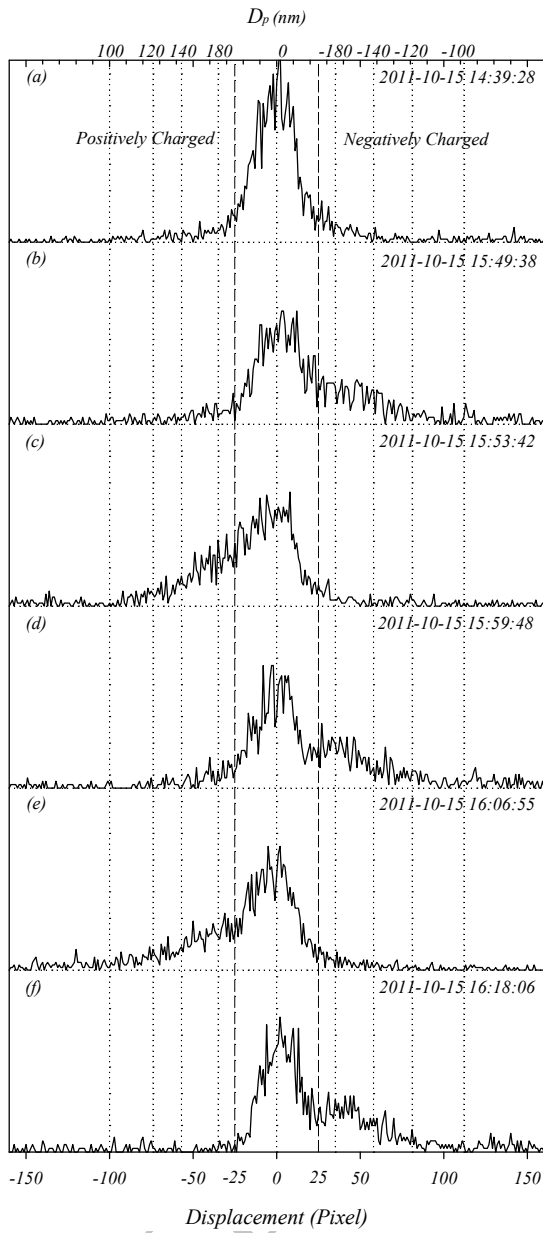
222 **Fig. 1.** The sampling location, Ansan, is located south-west of Seoul and near the Yellow Sea.

223



224

225 **Fig. 2.** Schematic of atmospheric particle sampling and measurement system.

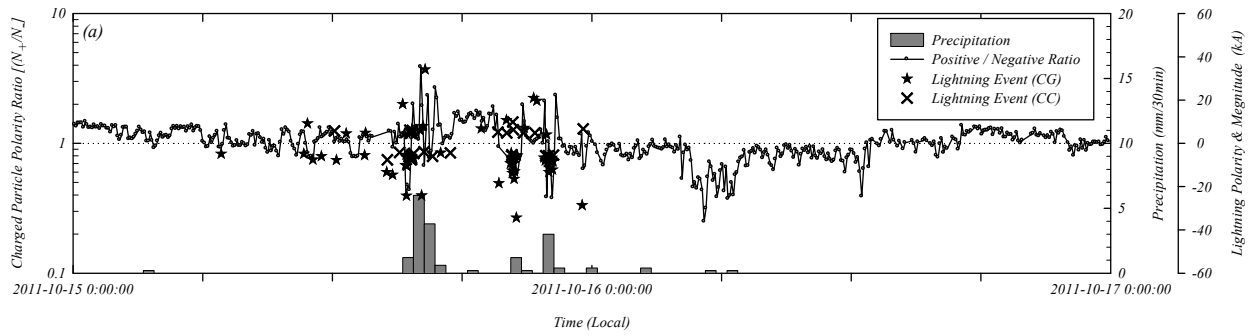


226

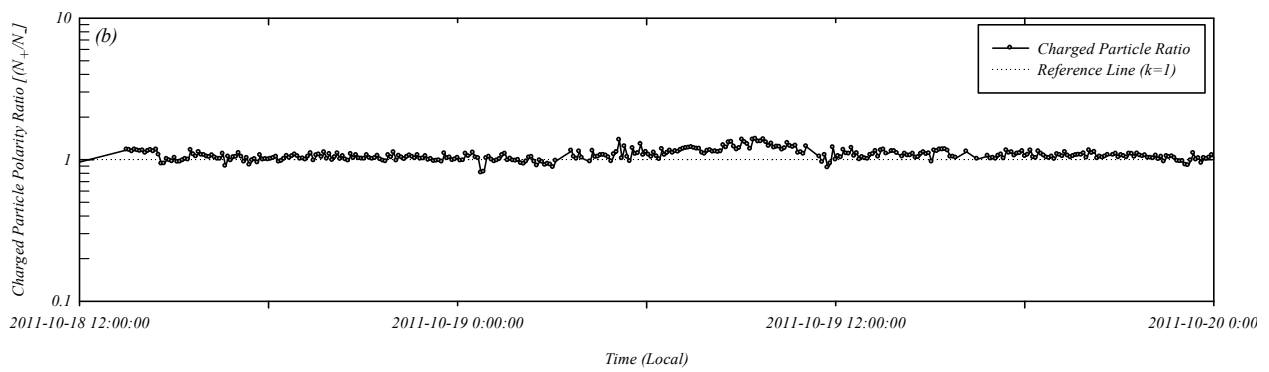
227 **Fig. 3.** Series of data measured by AEMSA. (a) Long before the rain accompanied by lightning.

228 (b), (c), (d), (e), (f) data are listed according to the lapses of time during lightning event.

229



230

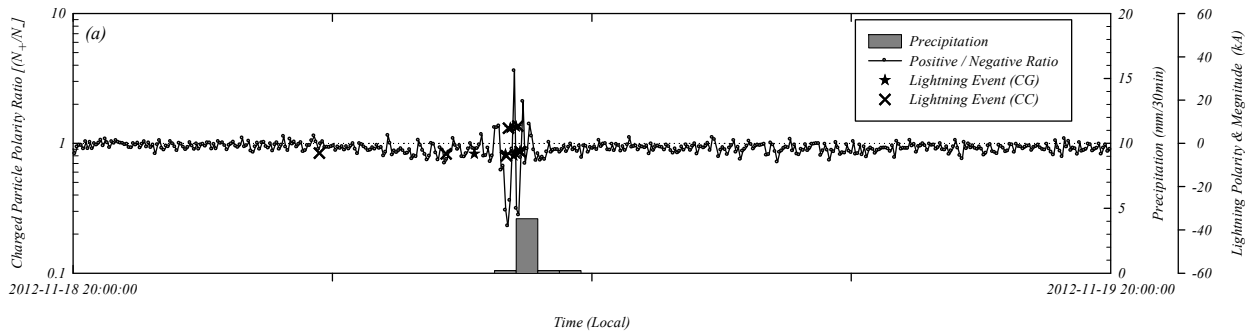


231

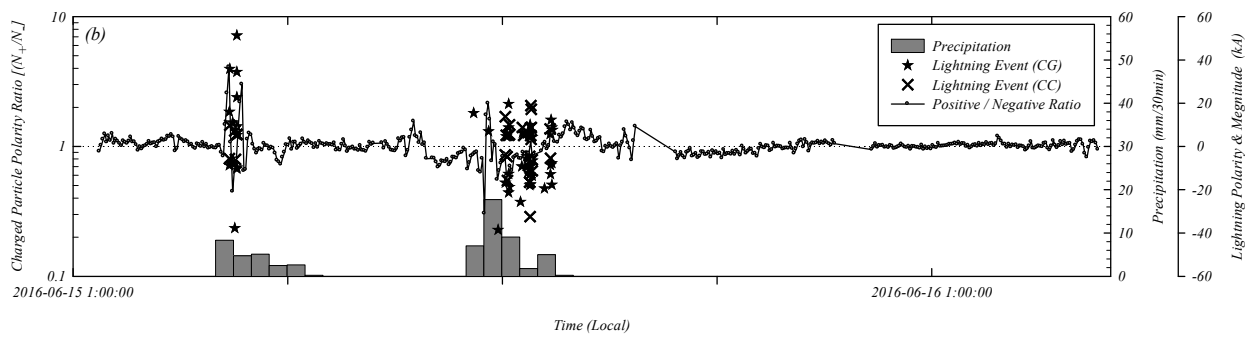
232 **Fig. 4.** The charged particle polarity ratio (N_+ / N_-) during (a) a lightning event and (b) clear days ;

233 (a) Oct. 15 – 16th, 2011, (b) Oct. 18 - 19th, 2011.

234



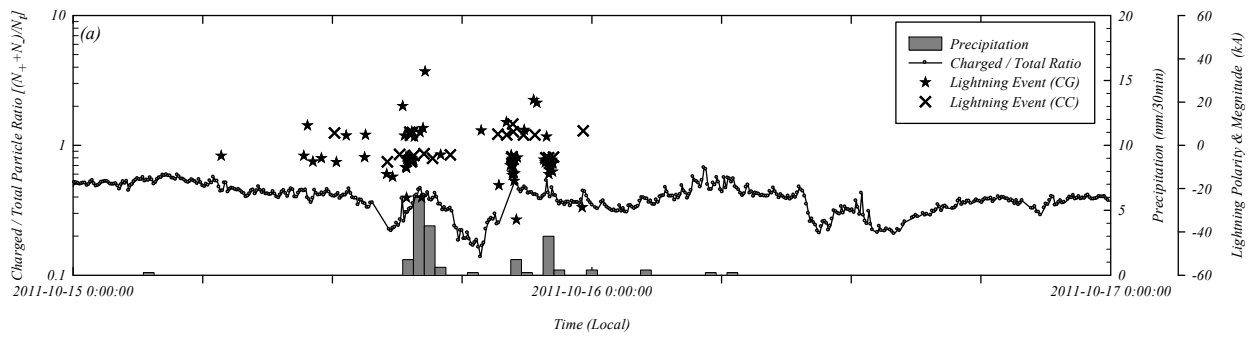
235



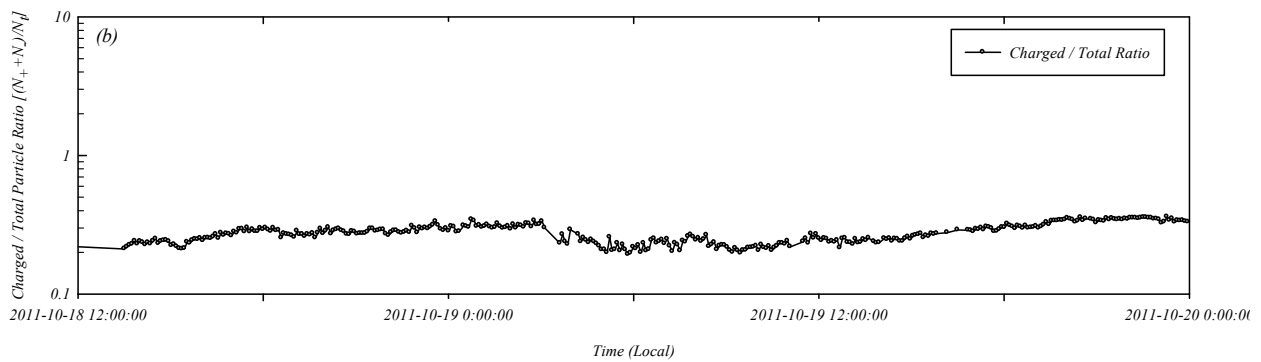
236

237 **Fig. 5.** The charged particle polarity ratio (N_+ / N_-) during lightning event ; (a) Nov. 18 – 19th,
 238 2012 (winter season), (b) Jun. 15 - 16th, 2016 (summer season).

239



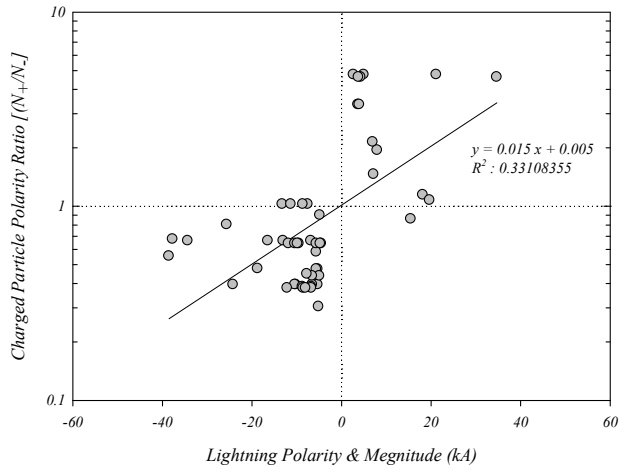
240



241

242 **Fig. 6.** The charged particle ($N_+ + N_-$) to total particle ($N_t = N_+ + N_- + N_0$) ratio during (a)
 243 lightning event and (b) clear days; (a) Oct. 15 - 16th, 2011, (b) Oct. 18 (cloud coverage: 0) - 19th
 244 (cloud coverage: 1.1), 2011.

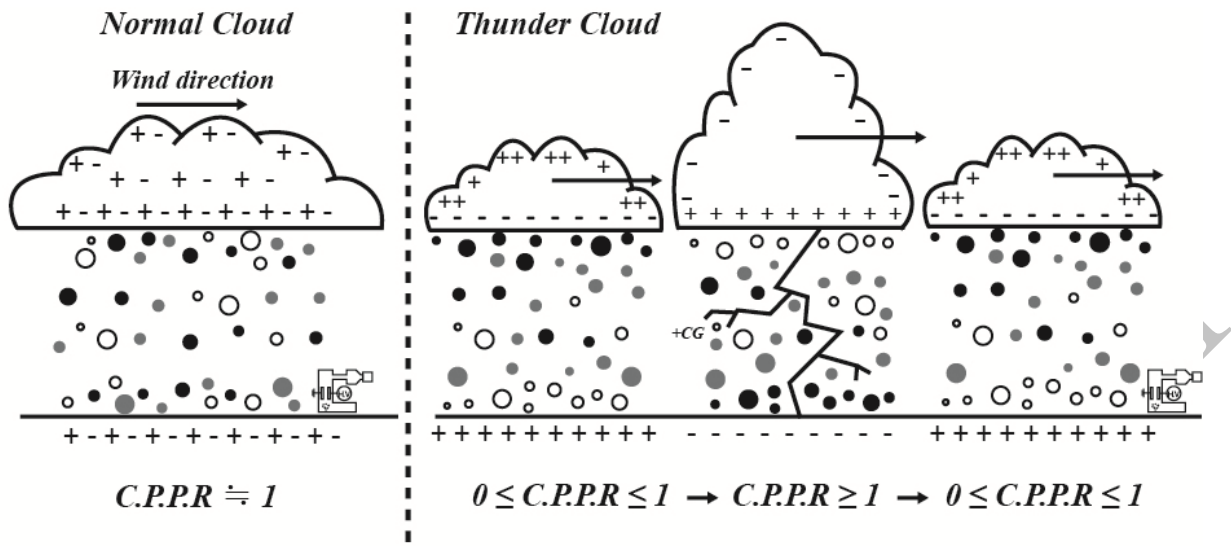
245



246
 247 **Fig. 7.** The charged particles polarity ratio according to lightning intensity during the CG
 248 lightning event measured from 2011 to 2016.

249

ACCEPTED MANUSCRIPT



C.P.P.R : Charged Particle Polarity Ratio (N^+ / N^-)

250 ● : Positively Charged Particle ○ : Negatively Charged Particle ◐ : Neutral Particle

251 **Fig. 8.** The mechanism of charged particle imbalance phenomenon

ACCEPTED MANUSCRIPT